CLUTTER REDUCTION IN ECHOCARDIOGRAPHY WITH SHORT-LAG SPATIAL COHERENCE (SLSC) IMAGING

Muyinatu A. Lediju Bell [⋆], *Robi Goswami* [†], *Gregg E. Trahey* [⋆‡]

[⋆]Duke University, Department of Biomedical Engineering, Durham, NC 27708, USA
[†]Duke University, Department of Cardiology, Durham, NC 27708, USA
[‡]Duke University, Department of Radiology, Durham, NC 27708, USA

ABSTRACT

Clutter, a problematic noise artifact in echocardiography, appears as a diffuse haze that obscures endocardial borders and inhibits accurate diagnoses. Several approaches are available to reduce clutter in cardiac images, yet difficult-to-image patients still exist. We have recently developed a novel imaging method, termed short-lag spatial coherence (SLSC) imaging, that has demonstrated potential to reduce clutter in simulated and experimental data. With this technique, images are created from the same individual channel signals used to form B-mode images, but instead of applying a conventional delay-and-sum beamformer, the data are cross-correlated to measure and display differences in spatial coherence. This technique was applied to *in vivo* cardiac images. Individual channel signals were acquired to form matched B-mode and SLSC images of the left ventricle in fourteen human volunteers. The contrast and contrast-to-noise ratio (CNR) of the ventricle and the signal-to-noise ratio (SNR) of the endocardium were measured in the same locations in matched B-mode and SLSC images. In SLSC images created with a short-lag value equivalent to 16% of the transmit aperture, contrast and CNR was improved by 9 ± 7 dB and 0.4 ± 0.2, respectively, in the SLSC images. The average SNR of the endocardium was 1.7 ± 0.4 in the SLSC images and 1.8 ± 0.4 in the B-mode images. The presented approach demonstrates a new method for reducing clutter in cardiac images.

***Index Terms*—** ultrasound, cardiac imaging, noise reduction

1. INTRODUCTION

Clutter is one of the most problematic noise artifacts in echocardiography. It obscures endocardial borders and corrupts diagnostic information. It is reported as a major problem in several cardiac applications, including strain imaging [1] and manual border detection [2], where up to 30% of myocardial segments in a clinically-relevant group of patients were reported as unobservable due to clutter. Additionally, clutter inhibits visualization of tumors, vegetations, and other cardiac abnormalities [3, 4], and approximately 10-20% of patients have suboptimal echocardiograms due to clutter [4, 5]. Sources of cardiac clutter include reverberations and reflections from extracardiac off-axis structures such as the ribcage and lungs, as well as from intracardiac structures such as the chordae tendineae, valves, and myocardial walls.

A common approach to clutter reduction in cardiac images is the use of harmonic imaging. In this technique, the higher harmonics generated by non-linear wave propagation through tissue are imaged, rather than the first, or fundamental, harmonic of the the transmitted pulse. Factors that contribute to clutter reduction with harmonic imaging include underdeveloped non-linear waves near the transducer surface, minimal harmonic content in reverberant echoes, low amplitude harmonic signals from multiple scattering, and suppressed side and grating lobes [6, 7, 8, 9]. In several studies, the application of harmonic imaging lowered the percentage of patients with suboptimal images due to clutter from 45-51% to 11-24% [10, 11]. However, the existence of this subset of patients with suboptimal harmonic images indicates that the technique is not always effective at reducing clutter.

Other clutter reduction approaches include transesophogeal echocardiography (TEE) [9] and various filtering methods, such as stationary clutter rejection [12] and principal component analysis [13, 14]. Despite these advancements, filters have limited ability to remove high-velocity clutter, and TEE poses a discomfort to patients and is not recommended for routine clinical use, only in cases where transthoracic images are diagnostically inconclusive or impossible / difficult to acquire [15].

Short-lag spatial coherence (SLSC) imaging [16], a novel approach that utilizes the spatial coherence of backscattered ultrasound echoes, is a competitive alternative to existing clutter reduction methods that overcomes many of the challenges with existing approaches. The spatial coherence of echoes from myocardium exhibits different characteristics from that of clutter and blood [17]. Since this difference is most noticeable for small spatial differences, SLSC imaging is im-

Special thanks to the UNCF-Merck Graduate Reseach Dissertation Fellowship, NIH Grant R37HL096023, and Dongwoon Hyun.

plemented by computing the spatial coherence of echoes at small spatial differences (i.e. for small, or short, distances of element separation). This method is described in more detail in Section 2. When compared to conventional B-mode images, SLSC images demonstrate superior contrast, SNR, and CNR in *in vivo* applications [16], particularly in the presence of acoustic noise (i.e. clutter) [18]. This is the first study to demonstrate the clutter reduction capabilities of SLSC imaging in echocardiography.

2. SHORT-LAG SPATIAL COHERENCE

To measure spatial coherence experimentally, the time-delayed echoes received by individual transducer elements are cross-correlated and plotted as a function of element separation (m). Due to signal non-idealities like clutter, aberration and thermal noise, experimental coherence functions do not always appear as predicted. The largest differences in spatial coherence occur in regions of low lags (i.e. when there is a small separation between elements). We define a metric, called the short-lag spatial coherence, that is the integral of the spatial coherence function over the first M lags, where M is a value that typically corresponds with 1-30% of the transmit aperture.

This is described mathematically with the following equations:

$$\hat{R}(m) = \frac{1}{N-m} \sum_{i=1}^{N-m} \frac{\sum_{n=n_1}^{n_2} s_i(n) s_{i+m}(n)}{\sqrt{\sum_{n=n_1}^{n_2} s_i^2(n) \sum_{n=n_1}^{n_2} s_{i+m}^2(n)}}, \tag{1}$$

$$R_{sl} = \sum_{m=1}^{M} \hat{R}(m). \tag{2}$$

where $\hat{R}(m)$ is the normalized spatial coherence measured across a receive aperture [19], N is the number of receive elements, $s_i(n)$ is the time-delayed signal received by the ith element at depth, or time, n, expressed in number of samples, and R_{sl} is the short-lag spatial coherence.

One pixel in a SLSC image is formed by computing the short-lag spatial coherence at one depth, n, of the channel signals, using a correlation kernel size ($n_2 - n_1$) of one wavelength. This process is repeated at numerous axial and lateral positions to create a SLSC image. Matched B-mode images are constructed by applying a conventional delay-and-sum beamformer to the same channel signals used to make SLSC images.

There is a trade-off among imaging performance metrics as a function of M. Generally, lateral resolution is improved, the signal-to-noise ratio (SNR) is degraded, and the contrast and contrast-to-noise ratio (CNR) increases then decreases as the value of M increases. A detailed analysis of these characteristic trends is discussed in [16].

3. METHODS

A Verasonic^{TM} ultrasound scanner (Redmond, WA) and a 64-element ATL P4-2 transducer were utilized to acquire *in vivo* cardiac ultrasound data of the left ventricle (short axis view) in 14 volunteers, after IRB approval and informed consent. The volunteers consisted of 5 Duke University employees and 9 patients scheduled for an echocardiogram at the Duke University Medical Center. Thrity-five frames of data were acquired at a rate of 7 frames per second, with an axial sampling frequency of 30 MHz and a transmit frequency of 2 MHz. The ultrasound echo data received by the 64 individual transducer elements was processed offline to create matched B-mode and SLSC images. SLSC images were created with $M = 10$.

Performance was evaluated by measuring the contrast (C) and CNR of the ventricle and the SNR of the endocardium in the same locations in matched B-mode and SLSC images, using the following equations:

$$\mathrm{C} = 20\log_{10}\left(\frac{S_e}{S_v}\right), \tag{3}$$

where S_v and S_e are the mean signals in the ventricle and endocardium, respectively.

$$\mathrm{CNR} = \frac{|S_v - S_e|}{\sqrt{{\sigma_v}^2 + {\sigma_e}^2}}, \tag{4}$$

where σ_v and σ_e are the standard deviations of signals in the ventricle and endocardium, respectively.

$$\mathrm{SNR} = \frac{S_e}{\sigma_e}. \tag{5}$$

All image processing and data analyses were performed with MATLAB (The Mathworks Inc., Natick, MA) software. With MEX files and a 3.5GHz processor, the time to calculate one SLSC image was $\sim$2s.

4. RESULTS

Matched B-mode and SLSC images of the left ventricle of one volunteer are shown in Fig. 1 (a) and (b), respectively. The left ventricular and adjacent right ventricular and atrial cavities in Fig. 1 (b) contain less clutter than the respective locations in the matched B-mode image. Observation of the cine loop revealed a reduction of both stationary and nonstationary clutter, for all frames of acquired data, particularly in the near-field region.

SLSC and traditional M-mode images were created from channel data by forming an image of the same lateral position as a function of time. The comparative M-modes in Fig. 1(c) reveal that the SLSC image clarifies the inferior endocardial border, while the pericardium and anterior endocardial border are well visualized.

The SLSC image was used to manually trace the endocardial border in the left ventricle shown in Fig. 1 (b). Contrast,

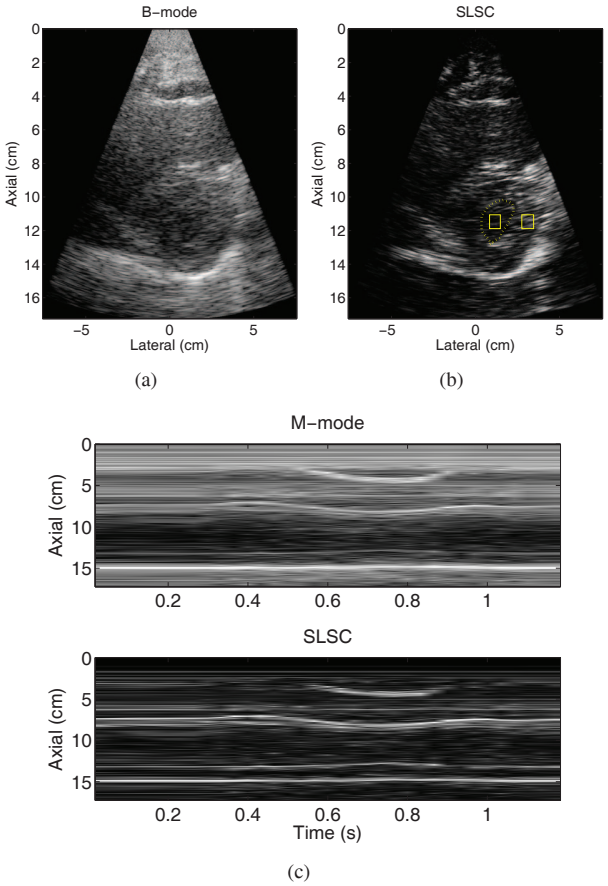

Fig. 1. Matched (a) B-mode and (b) SLSC images of the left ventricle of Volunteer 2. The endocardial border was manually outlined using visual inspection of a cine loop and the outlined ROIs were used to calculate contrast, CNR, and SNR. (c) Corresponding M-mode and SLSC images as a function of time.

CNR, and SNR, calculated with the boxes shown in Fig. 1 (b), measured 6.6 dB, 1.1, and 2.3, respectively, in the B-mode image and 9.1 dB, 1.1, and 2.0, respectively, in the SLSC image. Boxes in similar locations were used to calculate performance metrics for all of the volunteers.

Matched B-mode and SLSC images of the left ventricle from another volunteer are shown in Fig. 2 (a) and (b), respectively. Clutter is reduced and contrast is improved by approximately 7 dB in the SLSC image. CNR is improved by 0.5 and SNR is decreased by 0.6 in the SLSC image.

Fig. 3 shows the values of the contrast, CNR, and SNR of SLSC images plotted against those of B-mode images created from the same channel data for the fourteen volunteers. Values above the solid line indicate improvement with SLSC imaging. The contrast and CNR is improved in most SLSC images. The SNR variation is due to the large signal variation within the endocardiium, as demonstrated in Fig. 2.

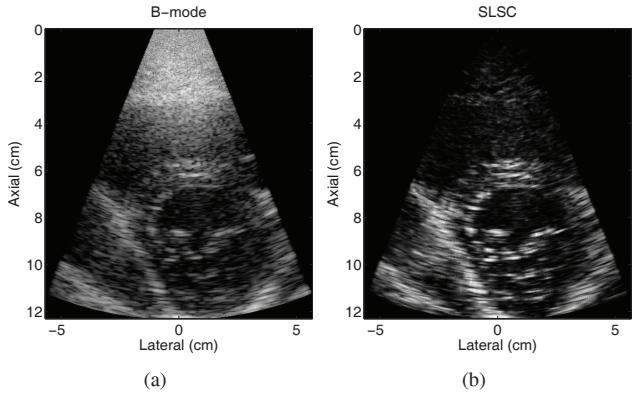

Fig. 2. Matched (a) B-mode and (b) SLSC images of the left ventricle of Volunteer 14.

5. DISCUSSION AND CONCLUSIONS

Examples of a difficult-to-image patient with conventional B-mode imaging (Fig. 1) are contrasted with examples from a less challenging patient (Fig. 2). The clutter is noticeably reduced in the SLSC images of all volunteers, compared to matched B-mode images, indicating the potential for SLSC imaging to reduce clutter in a range of patient types. These results demonstrate the potential for enhanced visualization of cardiac structures and abnormalities that are often obscured by the presence of clutter and offer preliminary evidence of improved endocardial border detection with SLSC imaging.

6. REFERENCES

[1] A.J. Teske, B.W.L. De Boeck, P.G. Melman, G.T. Sieswerda, P.A. Doevendans, and M.J.M. Cramer, "Echocardiographic quantification of myocardial function using tissue deformation imaging, a guide to image acquisition and analysis using tissue Doppler and speckle tracking," *Cardiovascular Ultrasound*, vol. 5, no. 1, pp. 27, 2007.

[2] D.G. Skolnick, S.G. Sawada, H. Feigenbaum, and D.S. Segar, "Enhanced endocardial visualization with noncontrast harmonic imaging during stress echocardiography," *Journal of the American Society of Echocardiography*, vol. 12, no. 7, pp. 559–563, 1999.

[3] A.K. Patel, A.V. Moorthy, V.U. Yap, and J.H. Thomsen, "Cardiac metastasis from transitional cell carcinoma: a subtle echocardiographic entity," *Journal of Clinical Ultrasound*, vol. 8, no. 1, 1980.

[4] D. Mele, O. Soukhomovskaia, E. Pacchioni, E. Merli, N. Avigni, L. Federici, R.A. Levine, and R. Ferrari, "Improved detection of left ventricular thrombi and spontaneous echocontrast by tissue harmonic imaging in pa-

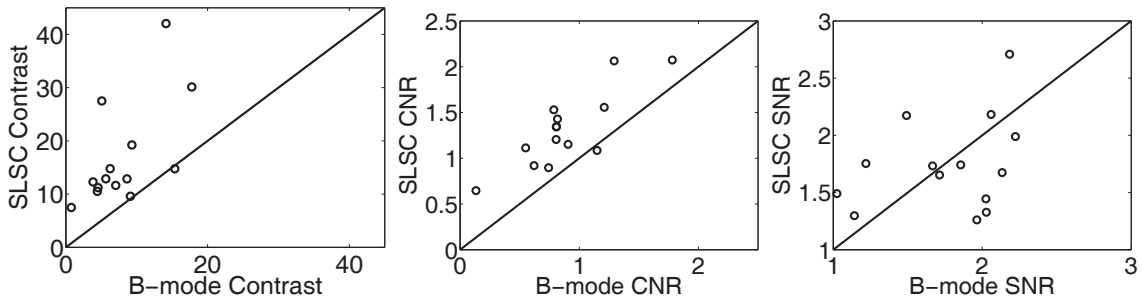

Fig. 3. Scatter plots of (a) contrast, (b) CNR, and (c) SNR measured in B-mode and SLSC images from the 14 volunteers. Data points above the solid line indicate better contrast, CNR, or SNR in the SLSC image compared to the matched B-mode image.

tients with myocardial infarction," *Journal of the American Society of Echocardiography*, vol. 19, no. 11, pp. 1373–1381, 2006.

[5] S.L. Mulvagh, A.N. DeMaria, S.B. Feinstein, P.N. Burns, S. Kaul, J.G. Miller, M. Monaghan, T.R. Porter, L.J. Shaw, and F.S. Villanueva, "Contrast echocardiography: current and future applications," *Journal of the American Society of Echocardiography*, vol. 13, no. 4, pp. 331–342, 2000.

[6] F. Tranquart, N. Grenier, V. Eder, and L. Pourcelot, "Clinical use of ultrasound tissue harmonic imaging.," *Ultrasound Med Biol*, vol. 25, no. 6, pp. 889–94, 1999.

[7] M.A. Averkiou, D.N. Roundhill, and J.E. Powers, "A new imaging technique based on the nonlinear properties of tissues," *Ultrasonics Symposium, 1997. Proceedings., 1997 IEEE*, vol. 2, pp. 1561–1566, October 1997.

[8] F. A. Duck, "Nonlinear acoustics in diagnostic ultrasound.," *Ultrasound Med Biol*, vol. 28, no. 1, pp. 1–18, 2002.

[9] B. Ward, Baker, and V.F. Humphrey, "Nonlinear propagation applied to the improvement of resolution in diagnostic medical ultrasound," *The Journal of the Acoustical Society of America*, vol. 101, no. 1, pp. 143–154, January 1997.

[10] F. Chirillo, A. Pedrocco, A. De Leo, A. Bruni, O. Totis, P. Meneghetti, and P. Stritoni, "Impact of harmonic imaging on transthoracic echocardiographic identification of infective endocarditis and its complications," *British Medical Journal*, vol. 91, no. 3, pp. 329–333, 2005.

[11] C. Caiati, N. Zedda, C. Montaldo, R. Montisci, and S. Iliceto, "Contrast-enhanced transthoracic second harmonic echo doppler with adenosine A noninvasive, rapid and effective method for coronary flow reserve assessment," *Journal of the American College of Cardiology*, vol. 34, no. 1, pp. 122–130, 1999.

[12] G. Zwirn and S. Akselrod, "Stationary clutter rejection in echocardiography," *Ultrasound Med Biol*, vol. 32, no. 1, pp. 43–52, Jan 2006.

[13] F. Mauldin, D. Lin, and J. Hossack, "The singular value filter: A general filter design strategy for pca-based signal separation in medical ultrasound imaging," *Medical Imaging, IEEE Transactions on*, , no. 99, pp. 1–1, 2011.

[14] M.A. Lediju, B.C. Byram, and G.E. Trahey, "Sources and characterization of clutter in cardiac b-mode images," in *Proceedings of the 2009 IEEE International Ultrasonics Symposium*, 2009, pp. 1419–1422.

[15] P. Hanrath, "Transoesophageal echo-Doppler in cardiology," *British Medical Journal*, vol. 86, no. 5, pp. 586–592, 2001.

[16] M. A. Lediju, G. E. Trahey, B. E. Byram, and J. J. Dahl, "Short-Lag Spatial Coherence of Backscattered Echoes: Imaging Characteristics," *IEEE Trans Ultrason, Ferroelec Freq Contr*, vol. 58, no. 7, pp. 1337, 2011.

[17] J.C. Bamber, R.A. Mucci, and D.P. Orofino, "Spatial Coherence and Beamformer Gain," *Acoustical Imaging*, vol. 24, pp. 43–48, 2000.

[18] JJ Dahl, D. Hyun, MA Lediju, and GE Trahey, "Lesion detectability in diagnostic ultrasound with short-lag spatial coherence imaging.," *Ultrason Imag*, vol. 33, no. 2, pp. 119, 2011.

[19] R. J. Fedewa, K. D. Wallace, M. R. Holland, J. R. Jago, G. C. Ng, M. R. Rielly, B. S. Robinson, and J. G. Miller, "Spatial coherence of the nonlinearly generated second harmonic portion of backscatter for a clinical imaging system," *IEEE Trans Ultrason, Ferroelec Freq Contr*, vol. 50, no. 8, pp. 1010–1022, 2003.